THE ASTRONOMICAL JOURNAL, 118:1061–1072, 1999 August

NEAR-SIMULTANEOUS SPECTROSCOPIC AND BROADBAND POLARIMETRIC OBSERVATIONS OF Be STARS

K. GHOSH,[1,2] K. V. K. IYENGAR,[3] B. D. RAMSEY,[1] AND R. A. AUSTIN[1]
Received 1998 August 7; accepted 1999 April 21

ABSTRACT

Near simultaneous optical spectroscopic (on four nights) and broadband linear continuum (B, V, R, and I bands) polarimetric (on seven nights) observations of 29 Be stars were carried out during 1993 November–December. The program Be stars displayed wavelength dependence of intrinsic polarizations with no frequency dependence of polarimetric position angles. Some of the Be stars displayed long-term polarization variability. The Be and Be-shell stars could not be distinguished from one another solely on the basis of their polarization values. Full widths at half-maximum of the Hα profiles and the intrinsic linear continuum polarizations are closely correlated with the projected rotational velocities of the program stars. Photospheric-absorption–corrected equivalent widths of Hα profiles [$W(\alpha)$] and the radii of Hα-emitting or -absorbing envelopes (R_e or R_a) are nonlinearly correlated with the intrinsic continuum polarizations of these stars. However, $W(\alpha)$ and R_e are linearly correlated. With large uncertainties, there is a trend of spectral dependence of polarization. Detailed discussion of these results is presented in this paper.

Key words: stars: emission-line, Be — techniques: polarimetric — techniques: spectroscopic

1. INTRODUCTION

Rapidly rotating B-type stars of luminosity classes III–V with Balmer emission lines are known as Be stars. Excess IR emission (Wright & Barlow 1975), optical and near-infrared emission-line profiles (details can be seen in Underhill & Dozan 1982), and ultraviolet wind lines (Snow 1981; Sonneborn et al. 1988; Grady et al. 1989, and references therein) have all been detected in Be stars. These results suggest the existence of extended circumstellar envelopes around these stars. Intrinsic linear polarization has been detected in Be stars. The measurements of linear polarizations of Be stars were started by Coyne & Gehrels (1967) and Coyne & Kruszewski (1969). It has been suggested that the linear polarizations of Be stars may be due to electron scattering in the inner regions of the equatorially flattened circumstellar envelopes (Coyne & Kruszewski 1969; Capps, Coyne, & Dyck 1973; Coyne 1976a, 1976b; McLean & Clarke 1976; Poeckert & Marlborough 1976; Wood, Bjorkman, & Bjorkman 1997, and references therein). Also, it has been reported that the polarizations in Be stars are variable on short to long timescales with constant polarimetric position angle, suggesting an axisymmetric geometry of the envelopes (Shakhovskoi 1965; McLean 1979; McLean & Clarke 1979; Hayes 1980; Bjorkman 1994). In general, it has been found that the maximum polarization exhibited by the Be stars is around 2% (Coyne & Gehrels 1967; Poeckert & Marlborough 1976; McLean & Brown 1978; Poeckert, Bastien, & Landstreet 1979; McDavid 1986, 1990, 1994, 1995; McDavid et al. 1996), an exception being γ Cas, which has displayed polarization as high as 2.5% (Coyne 1976a, 1976b; Poeckert & Marlborough 1977). These polarizations are frequency-dependent and are correlated with the rotational velocities of the Be stars. To explain this $\sim 2\%$ polarization limit, different models were constructed by varying the geometry of the envelopes of Be stars from a spherically symmetric "onion-like" geometry (Doazan & Thomas 1982) to an ellipsoidal geometry (Doazan 1987). However, VLA observations of ψ Per give direct evidence for flat envelopes of Be stars (Dougherty & Taylor 1992). Subsequent interferometric results also support the view that the equatorial envelopes of Be stars are flat (Quirrenbach et al. 1994a, 1994b, 1997). It has been found in many Be stars that the linear polarization of the star increases during the onset of its shell phase (McLean & Brown 1978; Arsenijevic, Jankov, & Djurasevic 1987). Probably during the Be-shell phase, the density of scatterers in the envelope increases, which in turn may increase the polarization of the shell stars. However, statistically it is not clear whether or not the Be-shell stars display higher polarizations than the Be stars.

Significant improvements in polarimetric modeling techniques of Be stars have been made in order to understand the geometry of Be star disks. Based on Monte Carlo modeling of optical continuum spectropolarimetry of Be stars, Wood et al. (1997) obtained two solutions, a geometrically thin and a geometrically thick disk. They have shown that the thin-disk solution is consistent with either a Keplerian or a wind-compressed disk (Bjorkman & Cassinelli 1993). Also, their thin-disk model can reproduce the multi-frequency (far-infrared through ultraviolet) continuum-energy distribution of Be stars. These results provide convincing evidence that the circumstellar disks of Be stars are geometrically thin (Wood et al. 1997). In addition, recent optical interferometric images and spectropolarimetric results of Be stars clearly exclude the geometrically thick-disk option for these stars and lead strongly to the conclusion that the envelope of Be stars are geometrically thin (Quirrenbach et al. 1997). Although now we have a better understanding of the geometry of the disk of Be

[1] NASA/Marshall Space Flight Center, Mail Code ES84, Space Sciences Laboratory, Huntsville, AL 35812; kajal.ghosh@msfc.nasa.gov, brian.ramsey@msfc.nasa.gov, robert.austin@msfc.nasa.gov.

[2] NAS/NRC Research Associate; on leave from the Indian Institute of Astrophysics, India.

[3] Indian Institute of Astrophysics, Bangalore 560034, India; kvki@iiap.ernet.in.

stars, it is still important to learn about the physical conditions (velocity, density, and temperature profile) in the disk. Such information may be obtained through simultaneous spectroscopic and polarimetric observations that will enable us to simultaneously probe the different physical regions and parameters of the disks of Be stars.

To find out the polarimetric properties of Be and Be-shell stars and also to search for a possible correlation between the linear polarization and the equivalent width of the Hα emission line, near-simultaneous spectroscopic and broad-band polarimetric observations of 29 Be stars were carried out. Results of these observations are presented in this paper. Section 2 describes the observations. Data analysis, results, and discussion are presented in § 3. Section 4 describes the conclusions.

2. OBSERVATIONS

The spectra of the program Be stars were obtained on four nights during 1993 November–December, using the Universal Astronomical Grating Spectrograph (UAGS) at the Cassegrain focus of the 1 m reflector of Vainu Bappu Observatory, Kavalur, India, and a few spectra were also obtained using the echelle spectrograph at the coudé focus of the same telescope, with a 254 mm camera and a CCD system. Iron-argon or iron-neon and thorium-argon source spectra were used for wavelength calibration. Dome flat-field frames were obtained to remove the pixel-to-pixel quantum efficiency variations. The reciprocal dispersions of the UAGS and echelle spectrographs are 19.6 Å mm^{-1} at Hα (0.45 Å pixel^{-1}) and 7.4 Å mm^{-1} at Hα (0.14 Å pixel^{-1}), respectively.

Polarimetric observations were carried out on seven nights, during 1993 November–December, using the star and sky chopping polarimeter (developed at the Indian Institute of Astrophysics; Jain & Srinivasalu 1991) attached at the f/13 Cassegrain focus of the 1 m reflector of VBO. A dry ice–cooled EMI 9658-R (extended S-20) photomultiplier tube coupled with the Fernie (1974) combination of glass filters [B (4400 Å/1050 Å), V (5425 Å/1050 Å), R (6550 Å/1300 Å), and I (8150 Å/1700 Å)] was used for the observations. The star and the neighboring sky, separated by about 2′, were observed alternately every 20 ms. This was done at 200 orientations of the analyzer. Typical integration times for the program Be stars were in the range of 6–10 minutes. An aperture of 15″ was used in all the observations. Polarimetric observations of each star were carried out on at least two nights, and each star was observed for at least 2–3 times on each night. Both polarized (Hsu & Breger 1982) and unpolarized standard stars (Serkowski 1974) were observed on each night to measure the zero correction of the position angle and the instrumental polarization, respectively.

3. DATA REDUCTIONS AND RESULTS

3.1. *Spectroscopic Data, Reductions, and Results*

Standard IRAF reduction packages and standard reduction techniques for CCD data were used to analyze the spectra. The error in wavelength calibration was around 0.05–0.10 Å. Each spectrum was normalized in three to four different ways, using different continuum-fitting functions (second or third order of SPLINE or LEGENDRE functions). Then these three or four spectra were averaged to obtain the final normalized spectrum. This helped to reduce the error in normalizations. Error in normalization is estimated to be around 2% of the local continuum. The instrumental broadening was measured by measuring the FWHM of the narrowest line of the comparison spectral lines, and this value of the FWHM was taken as the instrumental broadening of the spectrograph. The values of instrumental broadening for the UAGS and the echelle spectrographs are 0.5 and 0.2 Å, respectively, at Hα. These values were used to correct for instrumental broadening of the measured FWHM values of Be stars. The errors in equivalent width measurements were computed using the expression of σ(EW) given in Ghosh (1988). All the spectra were obtained, within at most 3 to 4 days of the polarimetric observations.

Table 1 shows the HD and the HR numbers and the designated name, the spectral type with reference, the visual magnitude, and the rotational velocity with reference, for each of the program Be stars. It can be seen from this table that the spectral types of these stars have been classified into three groups: B, Be, and Be-shell. This classification has been done using the Hα profiles of these stars, as discussed below. The spectra of 29 program Be stars, in the Hα region, are displayed in Figure 1. Close examination of Hα profiles of these Be stars reveals the following results:

1. No core-emission component is present in the Hα profile of four Be stars (HD 44506, HD 56014, HD 217675, and HD 224544) after subtracting the photospheric Hα absorption profile (the details of subtraction of photospheric absorption profile will be discussed below) from the observed Hα profiles. The residual Hα profile (observed Hα profiles minus the photospheric Hα absorption profiles) of HD 217675 shows the presence of deep and narrow absorption component and this star has been classified as a Be-shell star. The residual Hα profiles of HD 44506, HD 56014 and HD 224544 display weak core absorption and, most probably, very weak emission at the wings. We have classified these three stars as weak Be-shell stars.
2. Hα profiles of six Be stars (HD 21641, HD 25940, HD 30076, HD 32991, HD 41335, and HD 217891) are single-peaked and the Hα profiles of the remaining 19 Be stars are double-peaked. Among these 19 Be stars, only five Be stars (HD 22192, HD 22780, HD 23016, HD 43544, and HD 45542) have displayed narrow absorption line at the center of Hα profile. The sharp absorption line at the center of Hα profile of HD 45542 is due to the telluric line. The values of full width at half-maximum (FWHM) of the absorption lines at the center of Hα profiles of HD 22780, HD 23016, and HD 43544 are in the range of 170 to 200 km s^{-1}, which is much broader than the range of absorption-line FWHM values of Be-shell stars (50–75 km s^{-1}; Srinivasan 1998). Also from the residual Hα profiles (observed Hα profile minus the photospheric Hα absorption profile) we find that the absorption lines at the center of Hα profiles of these three stars are not very deep. Based on these results we suggest that the narrow central reversal feature at the emission peak of Hα profiles of HD 22780, HD 23016, and HD 43544 are not due to the shell absorption and these stars are not Be-shell stars. However, a narrow ($\sim$70 km s^{-1}) and relatively deep absorption line is present at the emission peak of Hα profile of HD 22192, and we classify this star as a Be-shell star. Finally we find that there are 24 Be stars, two Be-shell stars, and three weak Be-shell stars are present in our sample (Table 1).

TABLE 1

Program Be Stars for Spectroscopic and Polarimetric Observations

HD	HR	Name	Spectral Type	Spectral Type Reference	V mag[a]	$v \sin i$ (km s^{-1})	$v \sin i$ Reference
144	7	10 Cas	B9 IIIe	1	5.58	170	2
5394	264	γ Cas	B0 IVe	3	2.39	230	4
10516	496	ϕ Per	B2 Vpe	5	4.07	493	2
18552	894		B8 Vne	6	6.11	320	2
21641			B8.5 Ve	4	6.75	184	2
22192	1087	ψ Per	B5 Ve–shell	5	4.23	390	2
22780	1113		B7 Vne	5	5.55	360	2
23016	1126	13 Tau	B9 Vne	1	5.69	260	4
25940	1273	48 Per	B3 Ve	5	4.04	233	2
28497	1423		B2 Vne	7	5.60	340	2
30076	1508	56 Eri	B2 Ve	5	5.90	240	2
32991	1660	105 Tau	B2 Ve	5	5.92	220	2
35439	1789	25 Ori	B1 Vpe	3	4.94	327	2
37202	1910	ζ Tau	B4 IIIpe	5	3.03	310	2
37795	1956	α Col	B7 IVne	7	2.60	180	4
41335	2142		B2 Vne	5	5.21	414	2
42054	2170		B4 Vnne	8	5.83	220	4
43285	2231		B6 Ve	5	6.07	290	2
43544	2249		B2.5 Vne	5	5.92	300	4
44506	2288		B3 Ve–shell	7	5.53	211	2
45542	2343	ν Gem	B6 IIIe	5	4.14	220	2
47054	2418		B8 Ve	6	5.57	270	2
48917	2492	10 Cma	B2 Ve	7	5.20	200	4
56014	2745	27 Cma	B3 IIIe–shell[b]	8	4.65	200	2
58715	2845	β Cmi	B8 Ve	9	2.90	265	2
83953	3858		B5 Ve	7	4.77	330	2
217675	8762	o And	B6 IIIpe–shell	10	3.62	333	2
217891	8773	β Psc	B6 Ve	5	4.53	160	2
224544	9068		B6 IVe–shell[b]	5	6.52	260	(4)

[a] From Hoffleit & Jaschek 1982.

[b] Weak shell stars.

References.—(1) Cowley 1972; (2) Bernacca & Perinotto 1970; (3) Morgan, Code, & Whitford 1955; (4) Hoffleit & Jaschek 1982; (5) Lesh 1968; (6) Cowley et al. 1969; (7) Houk & Smith-Moore 1988; (8) Houk 1982; (9) Slettebak 1954; (10) Racine 1968.

To measure the true Hα emission strength of the program Be stars, it is important to correct the observed Hα profiles for the underlying photospheric absorption and for the central reversal at the emission peak. Corrections for the effects of photospheric absorption. were carried out in two ways: (1) theoretically and (2) observationally. Theoretically, we have computed the photospheric Hα profiles of B stars. To carry out such computations we need the values of the effective temperatures, masses, radii, bolometric magnitudes, and luminosities of main-sequence stars in the spectral range B0–B9. These values were collected from the literature, mainly from Popper (1980) and Harmanec (1988). The adopted parameters for the main-sequence B stars that we have collected are very similar to the adopted values of Slettebak, Collins, & Truax (1992). Using these parameters and also using the Kurucz (1994) model atmosphere code, we computed the theoretical photospheric Hα profiles of B stars of different spectral types, luminosities, and $v \sin i$ values. These theoretical Hα profiles of B stars may be used for underlying photospheric absorption corrections for the program Be stars.

Photospheric absorption can also be corrected by using observed Hα profiles of B stars. For this purpose, we observed 17 non–emission-line B stars of different spectral types and luminosity classes, using the same instrumentation that was used for the program stars. These spectra were rotationally broadened to correspond to the $v \sin i$ values of 29 Be stars. Rotationally broadened Hα profiles may also be used to correct for photospheric absorptions. Equivalent widths of theoretically computed and rotationally broadened observed Hα profiles of B stars were compared, and it was found that the differences in equivalent widths were in the range 0.3–0.6 Å. These results suggest that either theoretical or rotationally broadened observed Hα profiles can be used for photospheric absorption corrections. These photospheric Hα absorption profiles were subtracted from the observed Hα profiles of 29 Be stars. An example of such a correction is shown in Figure 2. The theoretical, photospheric Hα absorption profile is shown in Figure 2 (*bottom*) and is marked "Theoretical profile" (*smooth line*). The inner thin line is the observed profile. The theoretical profile has been subtracted from the observed profile, and the "subtracted profile" is shown as the thick line on top of the observed profile.

It has been found from Figure 1 that there are 19 Be stars with central reversal in the emission peak of the Hα profile (double-peak Hα profile). Correction for the central reversal in 19 Be stars has been done through extrapolation (Slettebak et al. 1992). The extrapolated profile is shown with a dashed line in Figure 2. Such correction for the central reversal is not required for the single-peak Hα profile. Corrected Hα profiles were used to measure the

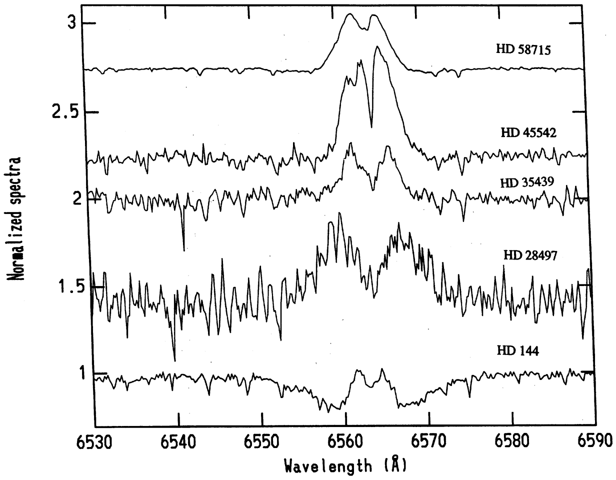

FIG. 1*a*

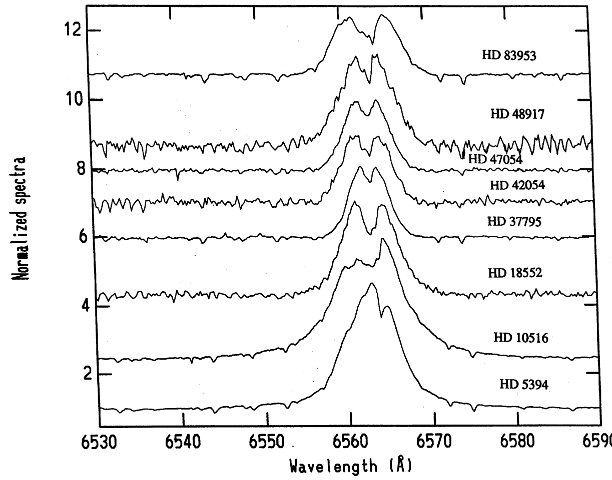

FIG. 1*b*

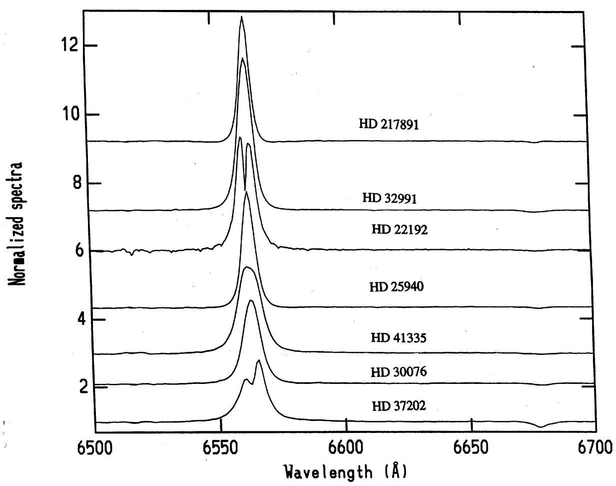

FIG. 1*c*

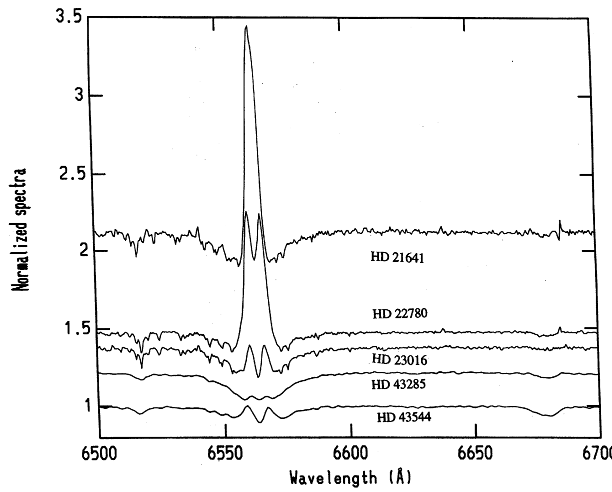

FIG. 1*d*

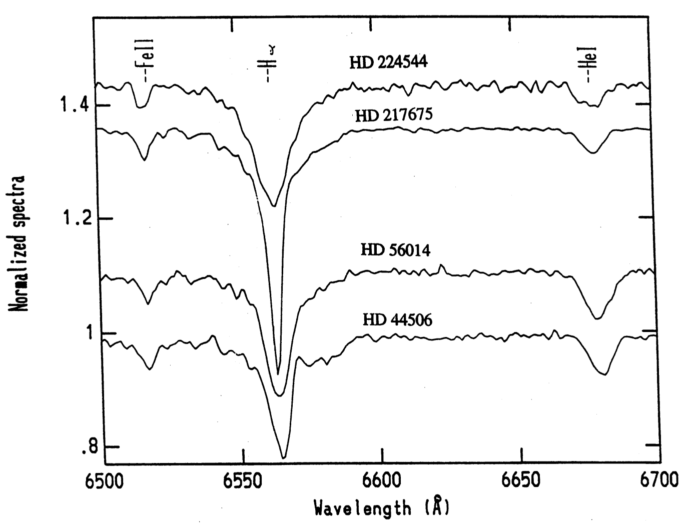

FIG. 1*e*

FIG. 1.—Normalized Hα profiles of 29 Be stars that were observed nearly with polarimetric observations. (*a* and *b*) Coudé echelle spectra of 13 Be stars. (*c*–*e*) Cassegrain spectra of the remaining 16 Be stars.

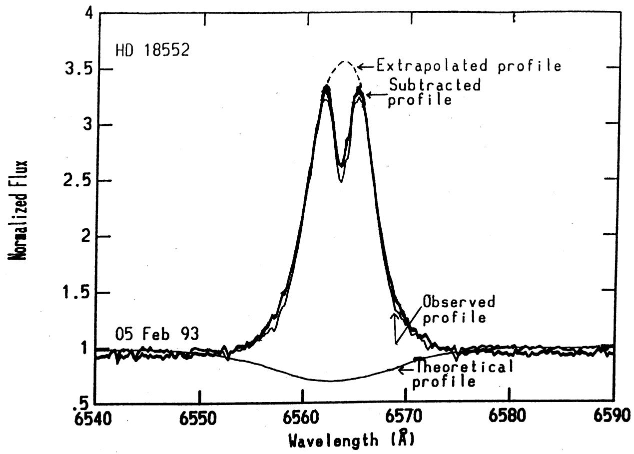

FIG. 2.—Examples of photospheric correction and artificial extrapolation of Hα profile of HD 18522. The smooth line is the theoretical profile. The inner thin line is the observed profile. The subtracted profile (the observed profile minus the theoretical profile) is shown as the thick line. The extrapolated profile (corrected for the central reversal) is shown as the dashed line.

FWHM and equivalent width values that are given in Table 2. Peak-separation (DV_{peak}) values were measured using the observed Hα profiles. These values of FWHM and DV_{peak} have been used to compute the radii of Hα-absorbing (R_a) and Hα-emitting envelopes (R_e), respectively, of the program Be stars. The radii of the envelopes of Be stars were computed using the following expressions (Huang 1972):

$$R_e = \left(\frac{2v \sin i}{\Delta V_{\text{peak}}}\right)^{1/j} R_* \quad \text{for emission-line stars}, \tag{1}$$

$$R_a = \left(\frac{2v \sin i}{\text{FWHM}}\right)^{1/(j+1)} R_* \quad \text{for absorption-line stars}, \tag{2}$$

where v is the equatorial stellar rotational velocity, $v \sin i$ is the projected rotational velocity of the star, ΔV_{peak} is the peak separation between the violet and red emission components of the Hα emission line, FWHM is the full width at half-maximum of the Hα shell-absorption component, j is an exponent that characterizes the rotation law ($j = 0.5$ for Keplerian rotation of the disk and $j = 1.0$ for rotation with conservation of angular momentum), and R_* is the stellar radius. Computed values of R_e and R_a (in units $R_\odot$) are given in Table 2 with probable errors.

3.2. *Polarimetric Data, Reductions, and Results*

The degrees of polarization and polarimetric position angle and their errors were measured by least-squares fitting to the intensity versus the angle data, after the sky background correction. The instrumental polarization was determined by repeated observations of several unpolarized

TABLE 2

MEASURED VALUES OF Hα PROFILES OF 29 Be STARS

HD	FWHM (km s^{-1})	ΔV_{peak} (km s^{-1})	EW(Hα)[a] (Å)	R_e or R_a ($R_\odot$)
144	218 ± 06	168 ± 07	02.07 ± 0.07	03.7 ± 0.3
5394	492 ± 09	146 ± 07	38.46 ± 1.88	33.1 ± 1.5
10516	520 ± 10	207 ± 09	45.17 ± 2.32	36.5 ± 2.5
18552	340 ± 08	157 ± 07	21.23 ± 1.45	15.6 ± 0.6
21641	238 ± 11	...	11.82 ± 0.38	...
22192[b]	376 ± 13	138 ± 08	35.61 ± 1.10	29.8 ± 1.4
22780	367 ± 11	200 ± 09	11.44 ± 0.45	16.2 ± 0.7
23016	342 ± 10	259 ± 10	05.74 ± 0.34	09.8 ± 0.6
25940	249 ± 11	...	24.15 ± 0.96	...
28497	299 ± 13	214 ± 09	07.97 ± 0.63	16.6 ± 0.9
30076	335 ± 12	...	24.85 ± 1.56	...
32991	294 ± 12	...	39.91 ± 1.72	...
35439	488 ± 14	312 ± 08	05.69 ± 0.43	15.7 ± 0.7
37202	455 ± 16	154 ± 10	24.98 ± 1.20	29.0 ± 1.6
37795	242 ± 10	117 ± 06	09.62 ± 0.88	13.7 ± 0.6
41335	480 ± 14	230 ± 10	37.43 ± 1.55	30.3 ± 2.5
42054	298 ± 09	137 ± 08	12.75 ± 0.69	19.0 ± 1.5
43285	415 ± 13	271 ± 08	03.21 ± 0.28	08.0 ± 0.5
43544	490 ± 14	344 ± 10	06.23 ± 0.45	09.7 ± 0.4
44506[c]	334 ± 11	...	−01.65 ± 0.04	07.3 ± 0.3[d]
45542	309 ± 09	134 ± 05	07.94 ± 0.73	12.6 ± 0.7
47054	276 ± 08	115 ± 05	11.32 ± 0.80	15.9 ± 1.4
48917	314 ± 10	121 ± 06	25.61 ± 0.94	26.0 ± 1.7
56014[c]	443 ± 12	...	−01.13 ± 0.06	03.7 ± 0.4[d]
58715	299 ± 11	145 ± 05	07.64 ± 0.67	12.0 ± 0.6
83953	399 ± 12	167 ± 07	11.41 ± 0.83	15.8 ± 0.8
217675[b]	251 ± 08	...	−02.48 ± 0.04	05.3 ± 0.3[d]
217891	202 ± 08	...	21.45 ± 1.56	...
224544[c]	498 ± 14	...	−02.07 ± 0.03	03.6 ± 0.3[d]

[a] Corrected for photospheric and shell absorption.
[b] Shell stars.
[c] Weak shell stars.
[d] Radius of Hα-absorbing envelope.

standard stars on each night. The value of the mean instrumental polarization was found to be 0.10%, and this value was almost constant during the interval of our observations (on seven nights during 1993 November–December). The instrumental polarization ($\sim 0.1\%$) was vectorially subtracted from the measured polarization of the program stars. The intrinsic polarization and polarimetric position angle were computed after removal of the interstellar polarization. The values of interstellar polarization in different filters were obtained from McLean & Clarke (1979) and Pockert et al. (1979). The interstellar polarization component was removed through a Serkowski-law fit and then vectorially subtracted using values in each filter. Values of probable errors associated with intrinsic polarization and position angle of the program stars were computed in two ways: (1) according to photon statistics and (2) based on multiple measurements. Usually it has been found that the computed values of probable errors based on multiple measurements are larger than that obtained from photon statistics, and these values of probable errors (based on multiple measurements) are listed in Table 2.

The measured average intrinsic polarizations (polarization measurements of each star were carried out on at least two nights and each star was observed for at least 2–3 times on each night) of the program stars in the *B*, *V*, *R*, and *I* bands with the probable errors are presented in Table 3. It may be seen from this table that six Be stars, including a Be-shell star (HD 22192), displayed polarizations (in the *B* band) between 0.94% and 1.57%. The percent of polarization of 19 program stars was around 0.5%, and the remaining four Be stars, including two weak Be-shell stars (HD 56014 and HD 224544), were in low polarization states ($\sim 0.25\%$). From these results (Table 3) we do not find any distinction in polarization level between Be and Be-shell stars. Polarization variability is quite common in Be stars (Bjorkman 1994; McDavid 1994). However, during the interval of our observations of these 29 Be stars, we could not detect any short-term variations (night to night) in the polarization levels of these stars. To search for long-term polarimetric variations of these stars, we compared our results with the published data. Figure 3 shows show the plots of the *B*-, *V*-, *R*-, and *I*-band polarizations versus dates of observations for HD 5394, HD 10516, HD 25940, HD 37202, and HD 217675. Polarimetric data of these five Be stars, between 1984 December and 1993 January, have been obtained from the published data by McDavid (1986, 1990, 1994) and are compared with our results in Figure 3. It can be seen from these plots that HD 5394, HD 10516, HD 25940, and HD 37202 displayed large amplitude polarimetric variations between 1993 January and December. HD 5394 displayed an almost constant level of polarization ($P^B \sim 0.75\% \pm 0.08\%$) between 1986 and 1992, but this level increased to $1.2\% \pm 0.1\%$ between 1992 and 1994. Figure 3*b* shows weak polarization variations of HD 10516 between 1985 and 1994. The polarization level of HD 25940 started declining in 1991, and this star exhibited almost

TABLE 3

MEASURED INTRINSIC POLARIZATIONS OF PROGRAM BE STARS

HD	POLARIZATION (%) *B*	*V*	*R*	*I*	P.A. (deg)
144	0.20 ± 0.06	0.16 ± 0.05	0.10 ± 0.05	0.12 ± 0.05	31 ± 2
5394	1.18 ± 0.10	0.89 ± 0.07	0.72 ± 0.05	0.58 ± 0.05	105 ± 4
10516	1.57 ± 0.11	1.36 ± 0.10	1.19 ± 0.09	0.98 ± 0.08	27 ± 2
18552	0.47 ± 0.05	0.38 ± 0.05	0.29 ± 0.05	0.17 ± 0.05	104 ± 5
21641	0.39 ± 0.06	0.26 ± 0.05	0.19 ± 0.06	0.12 ± 0.06	129 ± 8
22192[a]	0.94 ± 0.06	0.72 ± 0.05	0.54 ± 0.04	0.37 ± 0.04	43 ± 3
22780	0.57 ± 0.05	0.44 ± 0.05	0.30 ± 0.04	0.17 ± 0.04	106 ± 9
23016	0.45 ± 0.04	0.36 ± 0.04	0.25 ± 0.04	0.17 ± 0.04	169 ± 9
25940	0.69 ± 0.06	0.55 ± 0.05	0.44 ± 0.05	0.28 ± 0.04	140 ± 4
28497	0.61 ± 0.06	0.48 ± 0.05	0.32 ± 0.04	0.23 ± 0.04	114 ± 8
30076	0.64 ± 0.07	0.48 ± 0.05	0.32 ± 0.05	0.24 ± 0.05	115 ± 7
32991	1.38 ± 0.09	1.19 ± 0.09	1.06 ± 0.08	0.84 ± 0.07	68 ± 4
35439	0.51 ± 0.08	0.38 ± 0.07	0.26 ± 0.05	0.17 ± 0.05	108 ± 6
37202	1.03 ± 0.09	0.85 ± 0.08	0.73 ± 0.09	0.61 ± 0.08	35 ± 4
37795	0.34 ± 0.06	0.28 ± 0.05	0.21 ± 0.05	0.16 ± 0.05	77 ± 4
41335	1.02 ± 0.11	0.86 ± 0.11	0.71 ± 0.09	0.54 ± 0.08	148 ± 6
42054	0.39 ± 0.05	0.28 ± 0.05	0.19 ± 0.04	0.11 ± 0.04	82 ± 7
43285	0.45 ± 0.06	0.36 ± 0.07	0.24 ± 0.07	0.16 ± 0.06	52 ± 5
43544	0.48 ± 0.07	0.37 ± 0.06	0.26 ± 0.07	0.18 ± 0.05	44 ± 5
44506[b]	0.55 ± 0.07	0.39 ± 0.05	0.24 ± 0.05	0.13 ± 0.05	92 ± 7
45542	0.51 ± 0.08	0.40 ± 0.06	0.31 ± 0.06	0.19 ± 0.05	37 ± 5
47054	0.47 ± 0.05	0.34 ± 0.05	0.24 ± 0.05	0.17 ± 0.05	71 ± 6
48917	0.62 ± 0.09	0.51 ± 0.09	0.37 ± 0.07	0.24 ± 0.06	18 ± 5
56014[b]	0.21 ± 0.06	0.17 ± 0.05	0.11 ± 0.05	0.10 ± 0.05	82 ± 6
58715	0.36 ± 0.07	0.27 ± 0.07	0.18 ± 0.07	0.13 ± 0.05	90 ± 6
83953	0.54 ± 0.07	0.41 ± 0.08	0.30 ± 0.07	0.17 ± 0.05	95 ± 5
217675[a]	0.45 ± 0.07	0.38 ± 0.07	0.26 ± 0.06	0.19 ± 0.06	110 ± 8
217891	0.23 ± 0.07	0.17 ± 0.06	0.11 ± 0.05	0.09 ± 0.05	115 ± 7
224544[b]	0.25 ± 0.07	0.19 ± 0.08	0.12 ± 0.07	0.10 ± 0.06	90 ± 6

[a] Shell stars.

[b] Weak shell stars.

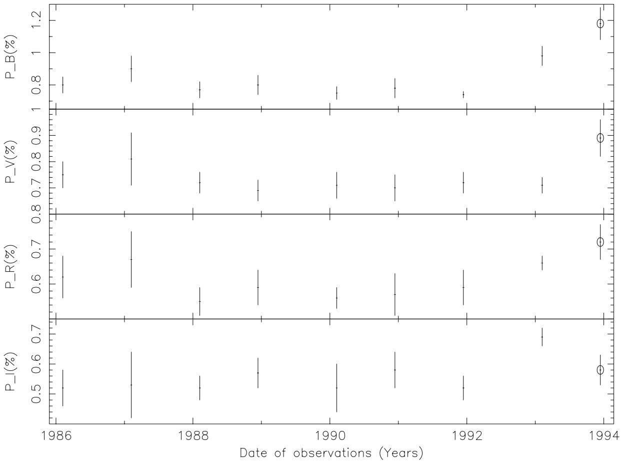

FIG. 3*a*

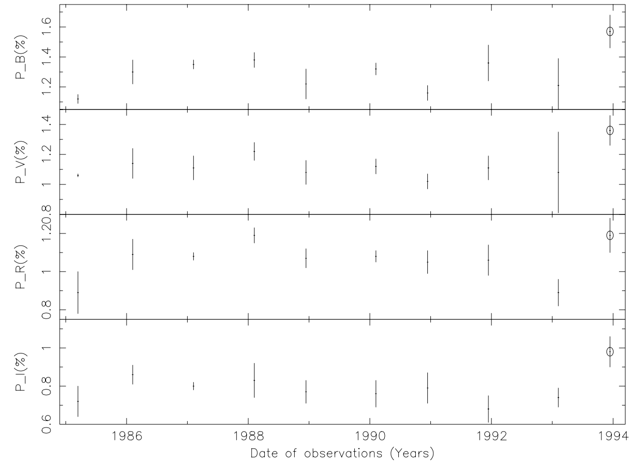

FIG. 3*b*

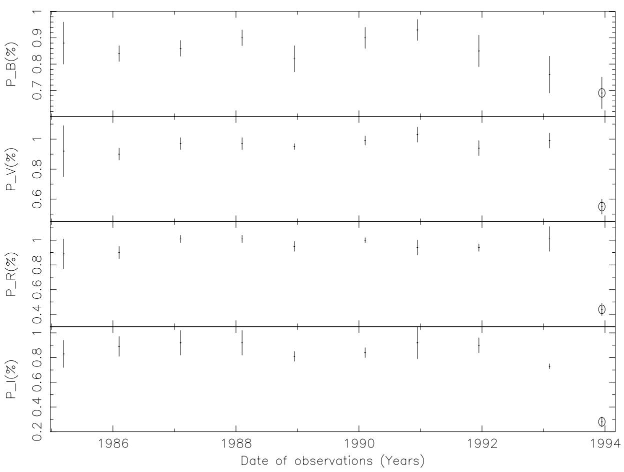

FIG. 3*c*

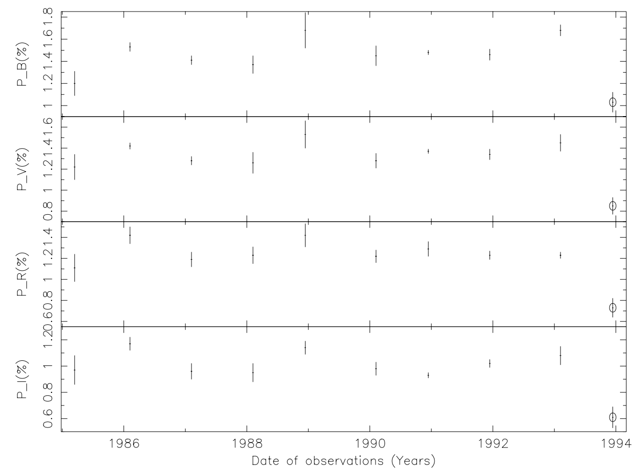

FIG. 3*d*

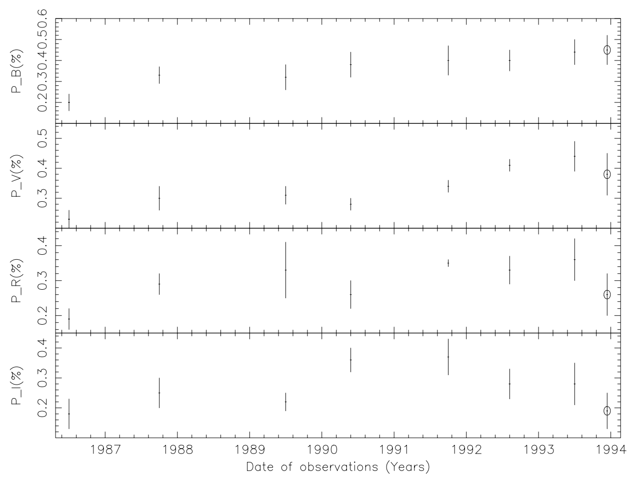

FIG. 3*e*

FIG. 3.—Measured polarization vs. date of observations for (*a*) HD 5394, (*b*) HD 10516, (*c*) HD 25940, (*d*) HD 37202, and (*e*) HD 217675. The four panels in each figure, from the top, are for polarizations in the *B*, *V*, *R*, and *I* filters. The *x*-axis represents the date of the observations in years, and the year labels are located at the beginning of the year. Data points with circles are from Table 3 of the present paper, and the remaining data points are from McDavid (1986, 1990, 1994).

constant polarization between 1985 and 1991; a similar pattern of variations has been found in HD 37202. HD 217675 (Be-shell star) did not vary during 1993 January–December. However, the B-band polarization of this star decreased by 0.6% between 1978 and 1984 (Pockert et al. 1979; McDavid 1986) and by 0.25% between 1984 December and 1993 December. We also compared our results with that obtained by Pockert et al. (1979) and found that the B-band polarizations of HD 22192 and HD 28497 decreased by 0.1% and 0.74%, respectively, and those of HD 30076, HD 32991, HD 41335, HD 45542, HD 58715, and HD 83953 increased by 0.44%, 0.65%, 0.62%, 0.31%, 0.26%, and 0.44%, respectively. These results support the earlier suggestion that Be stars are polarization-variable (Bjorkman 1994; McDavid 1994, and references therein).

We also measured the polarimetric position angles of 29 Be stars, and, from these measurements, we did not find any appreciable variations at different bands or wavelengths. Average values of position angles are given in Table 3, along with the probable errors. The polarimetric position angle is set by the orientation of the disk, and, if the polarization is due to electron scattering modified by hydrogen opacity in the circumstellar disk of Be stars, then the polarimetric position angle will be independent of wavelength (Coyne & Kruszewski 1969; McLean & Clarke 1979; Hayes 1980; Bjorkman 1994; Wood et al. 1997, and references therein). Our result that shows the lack of wavelength dependence of the polarimetric position angle of 29 Be stars is thus consistent with the previously published results by different investigators.

Measured polarizations of 29 Be stars (Table 3) are plotted in Figure 4. This figures show the wavelength dependence of polarization in these stars. It may be seen from these figures that the wavelength dependence of polarization is almost similar for all the stars in the present sample. Similar results were also obtained by McDavid (1994) for a sample of eight Be stars. This can also be shown through the plot of normalized polarization (P^V/P^B, where P^B and P^V are the polarizations at the B and V filters, respectively) against P^B (Fig. 5). No correlation is evident from this figure between P^V/P^B and P^B. This indicates that the values of P^V/P^B (the normalized dependence of polarization) are almost similar for all of the 29 Be stars. Our present results, along with similar results reported previously by other investigators, indicate that the frequency dependence of polarization is probably almost similar for all the observed Be stars. If the polarizing mechanism of multiple electron scattering is wavelength-independent, the observed polarization wavelength dependence may be due to pre- and postscattering attenuation by opacity sources in the disk. In the optical band, these opacity sources are dominated by the continuum opacity due to hydrogen, so the optical continuum polarization will follow the hydrogen opacity curve (Wood & Bjorkman 1995; Wood et al. 1996a, 1996b, 1997). The lack of wavelength dependence of polarimetric position angles and the observed polarization wavelength dependence are consistent with previously suggested models for axisymmetric envelopes of Be stars (McLean 1979; McLean & Clarke 1979; Hayes 1980; Bjorkman 1994).

The Figure 6 (*top*) shows the plot of P^B versus $v \sin i$, and Figure 6 (*bottom*) shows the plot of normalized polarization versus $v \sin i$. From this figure, it can be seen that P^B is correlated with $v \sin i$ (the solid line shows the best correlation between P^B and $v \sin i$), but the normalized polarization is not correlated with $v \sin i$. These results agree well with those obtained by Brown & McLean (1977). They suggested that such relations between P^B and $v \sin i$ can be explained with the assumption that the Be stars have axisymmetric single-scattering envelopes. However, it is most likely that the disks of Be stars are optically thick that may lead to multiple electron scattering in the envelopes of these stars (Waters & Marlborough 1992; Bjorkman & Bjorkman 1994; Hillier 1994; Wood et al. 1996a). We will state below that the linear polarization is not only correlated with $v \sin i$, but also correlated with the Hα emission strength of these stars.

3.3. *Results and Discussion from Polarimetric and Spectroscopic Data*

FWHM values of Hα profiles and $v \sin i$ values are plotted in Figure 7. It may be seen from this figure that these two parameters are correlated (the solid line shows the best correlation between FWHM and $v \sin i$, the correlation coefficient, is 0.793). Already we have seen that the $v \sin i$ is also correlated with the linear polarization (P^B). These results again support the previously reported suggestion of a "flattened" disk–type structure of the Balmer-emitting envelopes of Be stars (McLean 1979; Dougherty & Taylor 1992; Quirrenbach et al. 1994a, 1994b, 1997).

Based on nonsimultaneous observations, McLean (1979) and Hirata & Kogure (1984) suggested that there may be a correlation between P^B and $W(\alpha)$, but the nature of the relation between these two parameters was unknown. It is important to mention here that Cotš & Waters (1987) found an interesting correlation between the 12 μm IR color excess and P^B. The triangle-like shape of the distribution of these two parameters may be used as an indicator to roughly estimate the inclination angles of the disks of Be stars, even though these two parameters were not observed simultaneously. From near-simultaneous spectroscopic and broadband polarimetric observations, the equivalent widths of Hα profiles [photospheric absorption corrected, $W(\alpha)$] and polarizations at the B, V, R, and I bands were measured. Figure 8 presents the plot of $W(\alpha)$ versus P^B. The best fit to the data is shown by the dashed line, and this fit indicates that a nonlinear correlation (from the F-test analysis, it has been found that the fit is significant at 99.9% level) is present between P^B and $W(\alpha)$ $\{P^B = 0.474 - 0.122W(\alpha) + 0.0008[W(\alpha)]^2\}$. We have also found a similar relation between P^B and R_e. A plot of R_e versus P^B is shown in Figure 9. It may be noted from this figure that these two parameters are nonlinearly correlated (F-test analysis shows that the correlation is at better than the 99.9% significance level) and is similar to that of $W(\alpha)$ and P^B. However, Figure 10 [plot of $W(\alpha)$ vs. R_e] shows that $W(\alpha)$ is linearly correlated with R_e. Quirrenbach et al. (1997) have also found, for seven Be stars, that the Hα-emitting disk size is linearly correlated with the Hα emission strength. Results obtained from the present sample, which contains a larger number of Be stars, support the view of Quirrenbach et al. (1997) that the larger the size of the Hα-emitting disk, the stronger the Hα emission.

Figures 8 and 9 show the nonlinear correlation between P^B and $W(\alpha)$ and between P^B and R_e, respectively. Close examination of the left sides of these two figures suggest that the values of P^B were almost constant (around 0.5%) when the values of $W(\alpha)$ and R_e ranged between −2.0–12.0 Å and

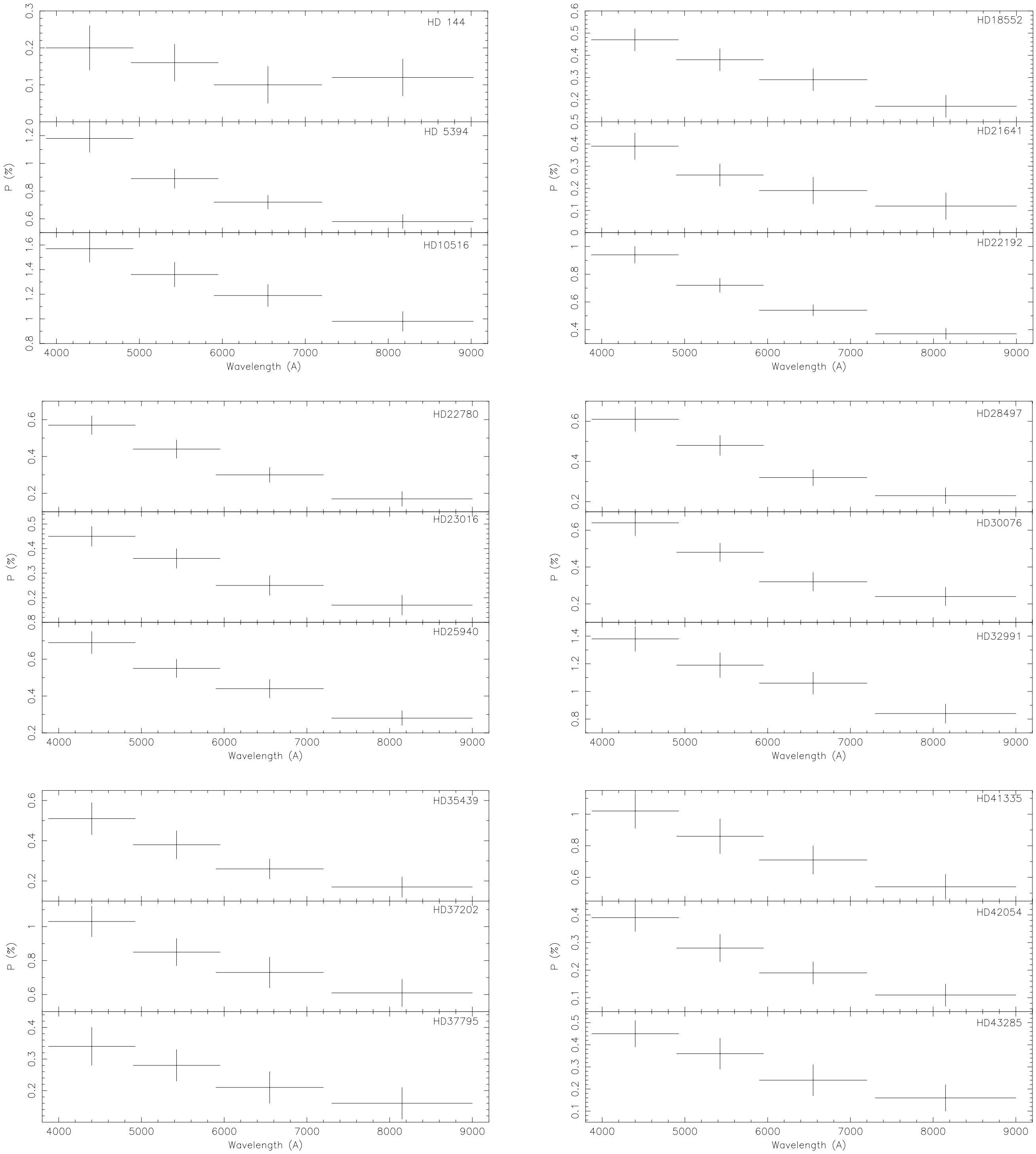

FIG. 4.—Intrinsic polarization as a function of wavelength for the program stars. The error bars represent the bandwidth in each filter for the wavelength scale and 1 σ uncertainties in polarization measurements

4.0–18 $R_\odot$, respectively. The right sides of these two figures show that the relations between P^B and $W(\alpha)$ and R_e were almost linear when the values of P^B, $W(\alpha)$, and R_e were in the ranges 0.5%–1.6%, 22.0–40.0 Å, and 26.0–36.0 $R_\odot$, respectively. Such relations may be explained using the emission-line wings of the Hα profiles of these stars. The full width at zero intensity (FWZI) is a measure of the extension of the emission-line wings. However, accurate measurement of FWZI requires high-resolution spectra of these stars. Also each spectra should cover at least 100–150 Å around Hα. We have obtained high-resolution spectra of 13 Be stars (Figs. 1*a* and 1*b*) that each covered only 75 Å around Hα. Spectra of the remaining 16 Be stars are low-resolution Cassegrain spectra (Figs. 1*c*–1*e*). Therefore, these spectra will not provide very accurate measurement of FWZI values (low-resolution spectra will introduce large uncertainties in measuring FWZI values). However, with all these uncertainties, we measured the FWZI values of Hα profiles of 29 Be stars. We find that the stars with $W(\alpha)$ values up to 12 Å have FWZI values in the range 13 ± 3 to 22 ± 4 Å

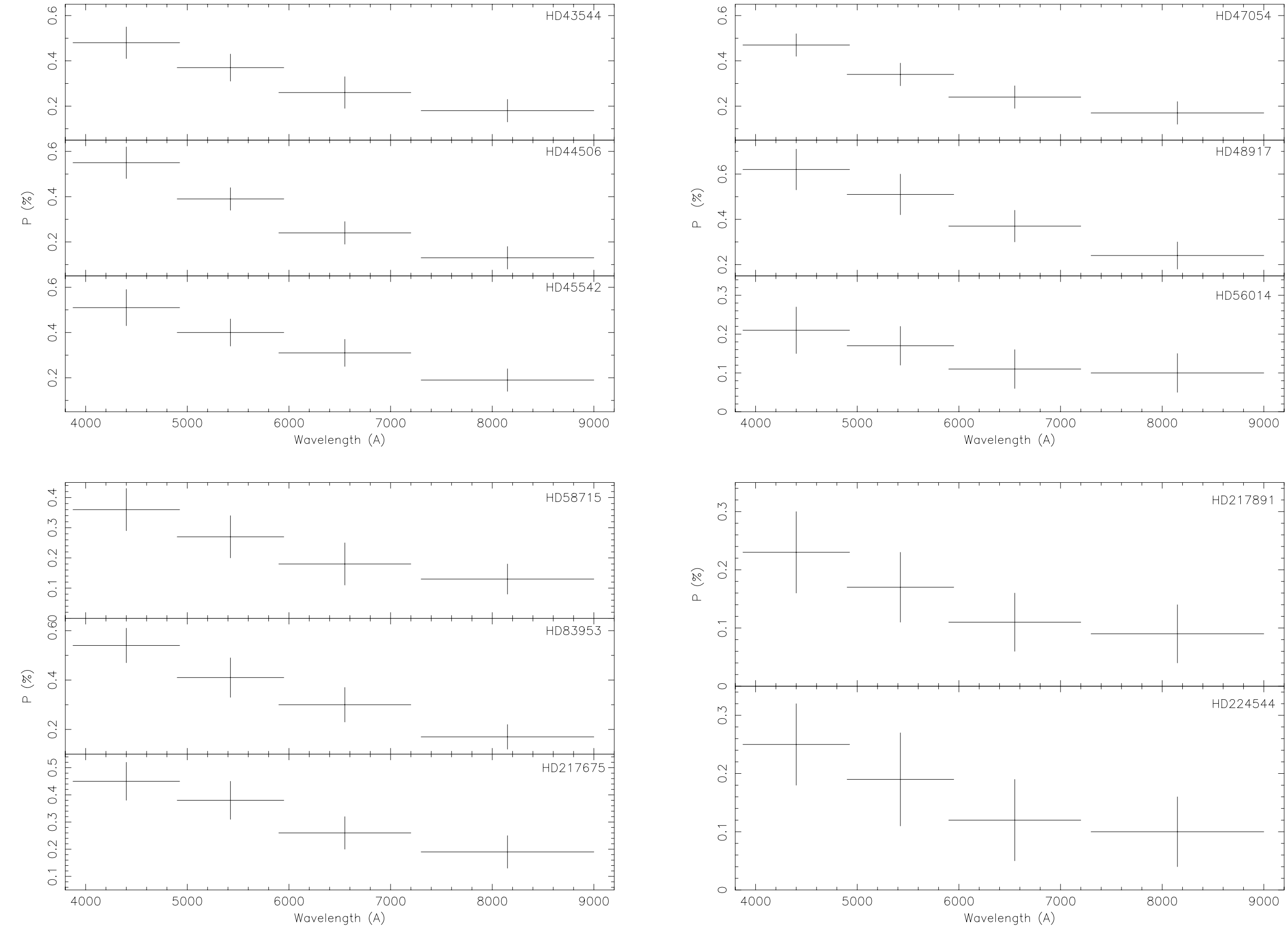

FIG. 4.—*Continued*

when the values of P^B are around 0.5%. Stars with $W(\alpha)$ values between 20 and 40 Å have very extended Hα profiles wings and FWZI values in the range 33 $\pm$ 4 to 55 $\pm$ 5 Å. All these stars with large $W(\alpha)$, R_e, and FWZI values have displayed high-level polarizations (the values of P^B were in the range 0.5%–1.6%). Recently McDavid, Bjorkman, & Baade (1999) have found an increase in polarization (P^B has increased from 0.23% to 0.56%) of *o* And (HD 217675) with the enhancement of emission-line wings of the Hα profiles, suggesting that the polarization is mainly due to electron scattering in the inner region of the envelope of the Be star. Our results also support this suggestion.

Values of P^B versus the spectral types of Be stars are plotted in Figure 11. The two solid lines in this figure show that all the stars except two (HD 23016 and HD 56014) lie within the triangular region in the P^B versus spectral type plane. The lower solid line suggest a weak correlation between these two parameters, and the upper line shows a strong dependence of P^B on the spectral type. In general (from Fig. 11) there is a trend that the Be stars of early spectral types have relatively larger polarizations than the

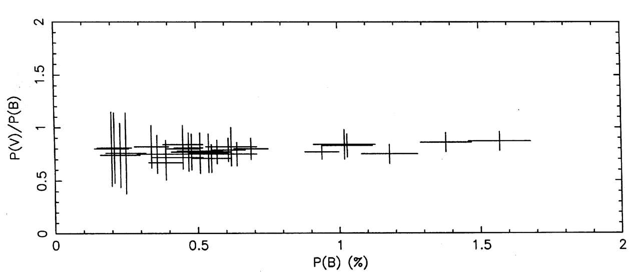

FIG. 5.—Plot of intrinsic polarization in the *B* band [$P(B)$] vs. the normalized polarization [$P(V)/P(B)$].

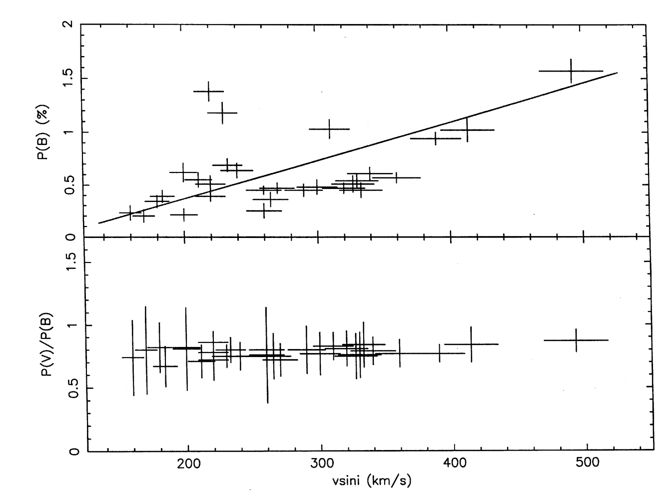

FIG. 6.—*Top*: Projected rotational velocities ($v \sin i$) of the program stars plotted against $P(B)$. The errors in $v \sin i$ are the 5% errors of the measured values of $v \sin i$. The 1 σ error bars are for P^B. The solid line shows the best-correlated fit between the two parameters. *Bottom*: $P(V)/P(B)$ vs. $v \sin i$.

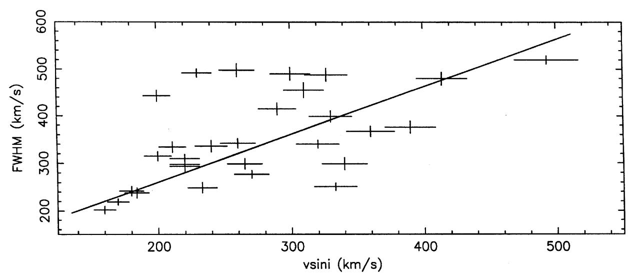

FIG. 7.—FWHMs of Hα profiles are plotted with $v \sin i$, and the solid line represents the best linear fit to the data. The 1 σ and 5% error bars are for FWHM and $v \sin i$, respectively.

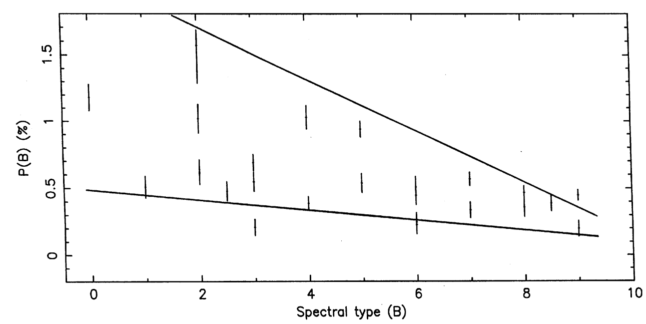

FIG. 11.—$P(B)$, with 1 σ error, as a function of spectral type for the program Be stars.

late-type ones. Usually the early spectral type Be stars will have more ionizing photon flux than the late-type Be stars. It is also known that the early-type Be stars (hotter Be stars) have higher electron densities in their envelopes than the late-type ones (cooler Be stars) (Slettebak et al. 1992). Since $W(\alpha)$ is proportional to N_e^2, it is expected that the early-type Be stars will usually produce larger Hα emissions than the late-type ones. If the polarization is due to multiple electron scattering with a frequency dependence due to absorption and emission by partially ionized hydrogen (Wood et al. 1996a, 1996b), then it is expected that the early-type Be stars will show larger polarizations. Figure 11 displays the same results. However, considering the uncertainties in spectral types for Be stars, the large errors in polarization measurements, and the small number of stars observed for the present study, it is suggested that this result (obtained from Fig. 11) is not statistically significant and should be used cautiously.

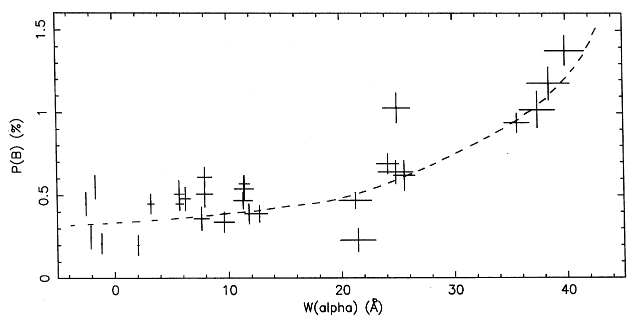

FIG. 8.—Plot of equivalent widths of Hα profiles [$W(\alpha)$] vs. $P(B)$ with 1 σ error bars. The best nonlinear fit to the data is shown by the dashed curve.

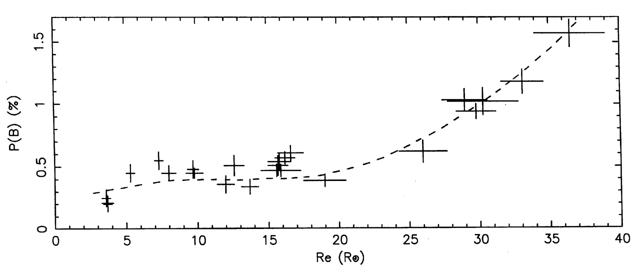

FIG. 9.—Computed radii of Hα-emitting/absorbing envelopes [R_e ($R_\odot$) or R_a ($R_\odot$)] of the program Be stars are plotted against $P(B)$ with 1 σ error bars. The dashed curve shows the best nonlinear fit to the data.

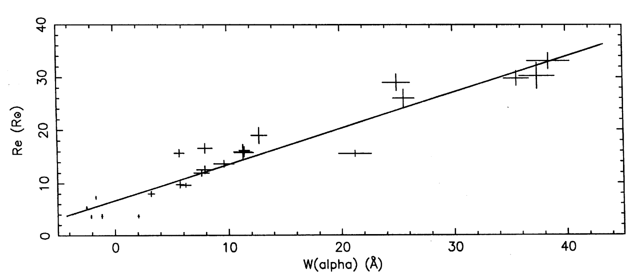

FIG. 10.—$W(\alpha)$ vs. R_e with 1 σ error bars. The best fit to the data is represented by the dashed line.

4. CONCLUSIONS

Based on the results obtained from near-simultaneous spectroscopic and polarimetric observations of 29 Be stars, the following conclusions may be drawn:

1. A wavelength dependence of the polarization but no frequency dependence of the polarimetric position angle was found for the 29 Be stars. The lack of correlation between P^B and the normalized polarization (P^V/P^B) suggests that the nature of the wavelength dependence of polarization is similar for all the Be stars. These results are consistent with previously reported results and suggest models with electron-scattering disks with attenuative hydrogen opacities, combined with dilution due to the visible central stars (Wood & Bjorkman 1995; Wood et al. 1996a, 1996b, 1997).

2. From the comparison of our results with the previously published data, it was found that many Be stars show long-term polarimetric variability, and this is consistent with the earlier reported results (Bjorkman 1994; McDavid 1994).

3. FWHMs of Hα profiles and intrinsic continuum polarizations are both closely correlated with the projected rotational velocities, $v \sin i$, of the program stars. However, no correlation is present between the normalized polarization (P^V/P^B) and the $v \sin i$ values. These results are consistent with previously suggested models for axisymmetric envelope of Be stars.

4. There are 24 Be stars and five Be-shell stars (three shell stars and two weak-shell stars) in the present sample. Measured polarization values of these stars (Table 3) do not display any distinction in polarization level between Be and Be-shell stars.

5. Photospheric-absorption–corrected equivalent widths of Hα profiles [$W(\alpha)$] and radii of Hα-emitting envelopes are nonlinearly correlated with P^B. However, $W(\alpha)$ and P^B are linearly correlated. These results are consistent with the suggestion that the polarization is mainly due to electron scattering in the inner region of the envelopes of Be stars (McDavid et al. 1999).

Our sincere thanks to the referee, K. S. Bjorkman, for her detailed and valuable comments and suggestions, which helped to improve this paper. We thank K. C. Srinivasan, R. Krishnamurthy, and K. R. Radhakrishnan for discussion. Our sincere thanks to K. Kuppuswamy, C. Velu, and A. Muniandi for their support and assistance during the observations. Also we thank S. Soundararajaperumal for his help in getting the plots. This work was performed while K. K. Ghosh held a National Research Council (NASA/Marshall Space Flight Center) Research Associateship.

REFERENCES

Arsenijevic, J., Jankov, S., & Djurasevic, G. 1987, in IAU Symp. 92, Physics of Be Stars, ed. A., Slettebak & T. P. Snow (Cambridge: Cambridge Univ. Press), 200
Bernacca, P. L., & Perinotto, M. 1970, Contr. Astrofys. Padova, 239, 1
Bjorkman, J. E., & Bjorkman, K. S. 1994, ApJ, 436, 818
Bjorkman, J. E., & Cassinelli, J. P. 1993, ApJ, 409, 429
Bjorkman, K. S. 1994, in IAU Symp. 162, Pulsation, Rotation, and Mass Loss in Early-Type Stars, ed. L. Balona, H. F. Henrichs, & J. M. LeContel (Dordrecht: Kluwer), 219
Brown, J. C., & McLean, I. S. 1977, A&A, 57, 141
Capps, R. W., Coyne, G. V., & Dyck, H. M. 1973, ApJ, 184, 176
Cotŝ, J., & Waters, L. B. F. M. 1987, A&A, 176, 93
Cowley, A. 1972, AJ, 77, 750
Cowley, A., Cowley, C., Jaschek, M., & Jaschek, C. 1969, AJ, 74, 375
Coyne, G. V. 1976a, A&A, 49, 89
———. 1976b, in IAU Symp. 70, Be and Be Shell Stars, ed. A. Slettebak (Dordrecht: Reidel), 233
Coyne, G. V., & Gehrels, T. 1967, AJ, 72, 887
Coyne, G. V., & Kruszewski, A. 1969, AJ, 74, 528
Doazan, V. 1987, in IAU Colloq. 92, Physics of Be Stars, ed. A. Slettebak & T. P. Snow (Cambridge: Cambridge Univ. Press), 384
Doazan, V., & Thomas, R. N. 1982, in B Stars with and without Emission Lines, ed. A. Underhill & V. Doazan (NASA SP-456) (Washington: NASA), 409
Dougherty, S. M., & Taylor, A. R. 1992, Nature, 359, 808
Fernie, J. D. 1974, ApJ, 188, 53
Ghosh, K. K. 1988, A&AS, 75, 261
Grady, C. A., Bjorkman, K. S., Snow, T. P., Sonneborn, G., Shore, S. N., & Barker, P. K. 1989, ApJ, 339, 403
Harmanec, P. 1988, Bull. Astron. Instit. Czechoslovakia, 39, 329
Hayes, D. P. 1980, PASP, 92, 661
Hillier, D. J. 1994, A&A, 289, 492
Hirata, R., & Kogure, T. 1984, Bull. Astron. Soc. India, 12, 109
Hoffleit, D., & Jaschek, C. 1982, The Bright Star Catalogue (New Haven: Yale Univ. Obs.)
Houk, N. 1982, Catalogue of Two-dimensional Spectral Types for the HD Stars, Vol. 3 (Ann Arbor: Univ. Michigan Dept. Astron)
Houk, N., & Smith-Moore, M. 1988, Catalogue of Two-dimensional Spectral Types for the HD Stars, Vol. 4 (Ann Arbor: Univ. Michigan Dept. Astron)
Hsu, J. C., & Breger, M. 1982, ApJ, 262, 732
Huang, S. S. 1972, ApJ, 171, 549
Jain, S. K., & Srinivasalu, G. 1991, Opt. Eng., 30, 1415
Kurucz, R. L. 1994, CD-ROM 19, Solar Model Abundance Model Atmospheres (Cambridge: Smithsonian Astrophys. Obs.)
Lesh, J. R. 1968, ApJS, 17, 371
McDavid, D. 1986, PASP, 98, 572
———. 1990, PASP, 102, 773
———. 1994, PASP, 106, 949
———. 1995, AAS, 186, 2211
McDavid, D., Bjorkman, K. S., & Baade, D. 1999, BAAS, 30, 1396
McDavid, D., Hirata, R., Guinan, E. F., Bjorkman, K. S., & Babler, B. L. 1996, BAAS, 28, 913.
McLean, I. S. 1979, MNRAS, 186, 265
McLean, I. S., & Brown, J. C. 1978, A&A, 69, 291
McLean, I. S., & Clarke, D. 1976, in IAU Symp. 70, Be and Be Shell Stars, ed. A. Slettebak (Dordrecht: Reidel), 261
———. 1979, MNRAS, 186, 245
Morgan, W. W., Code, A. D., & Whitford, A. F. 1955, ApJS, 2, 41
Poeckert, R., Bastien, P., & Landstreet, J. D. 1979, AJ, 84, 812
Poeckert, R., & Marlborough, J. M. 1976, ApJ, 206, 182
———. 1977, ApJ, 218, 220
Popper, D. M. 1980, ARA&A, 18, 115
Quirrenbach, A., Buscher, D. F., Hummel, C. A., Mozurkewich, D., & Armstrong, J. T. 1994a, A&A, 283, L13
Quirrenbach, A., Mozurkewich, D., Buscher, D. F., Hummel, C. A., & Armstrong, J. T. 1994b, A&A, 286, 1019
Quirrenbach, A., et al. 1997, ApJ, 479, 477
Racine, R. 1968, AJ, 73, 588
Serkowski, K. 1974, in Planets, Stars and Nebulae Studied with Photopolarimetry, ed. T. Geherls (Tucson: Univ. Arizona Press), 195
Shakhovskoi, N. M. 1965, Soviet Astron., 8, 833
Slettebak, A. 1954, ApJ, 119, 146
Slettebak, A., Collins, G. W., II, & Truax, R. 1992, ApJS, 81, 335
Snow, T. P. 1981, ApJ, 251, 139
Sonneborn, G., Grady, C. A., Wu, C.-C., Hayes, D. P., Guinan, E. F., Barker, P. K., & Henrichs, H. F. 1988, ApJ, 325, 784
Srinivasan, K. C. 1998, Ph.D. thesis, Bharathidasan Univ.
Underhill, A., & Doazan, V. 1982, in B Stars with and without Emission Lines (NASA SP-456) (Washington: NASA), 279
Waters, L. B. F. M., & Marlborough, J. M. 1992, A&A, 256, 195
Wood, K., & Bjorkman, J. E. 1995, ApJ, 443, 348
Wood, K., Bjorkman, K. S., & Bjorkman, J. E. 1997, ApJ, 477, 926
Wood, K., Bjorkman, J. E., Whitney, B. A., & Code, A. D. 1996a, ApJ, 461, 847
———. 1996b, in ASP Conf. Ser. 97, Polarimetry of the Interstellar Medium, ed. W. G. Roberge & D. C. B. Whittet (San Francisco: ASP), 191
Wright, A. E., & Barlow, M. J. 1975, MNRAS, 170, 41